Towards Eco-Friendly Waste Solutions: Environmental Impact of Engineered Cementitious Composites in Solid Waste Management

G. Muthumari[1], P. Vincent[2*], I. Baskar[3]

[1]Department of Civil Engineering, Mohamed Sathak Engineering College, Kilakarai - 623806, Tamil Nadu, India.

[2*,3]Department of Civil Engineering, Mepco Schlenk Engineering College, Sivakasi - 626005, Tamil Nadu, India.

[*]Corresponding Author:

E-mail: vincekavi1963@gmail.com, tel: +91-9443110487

GRAPHICAL ABSTRACT

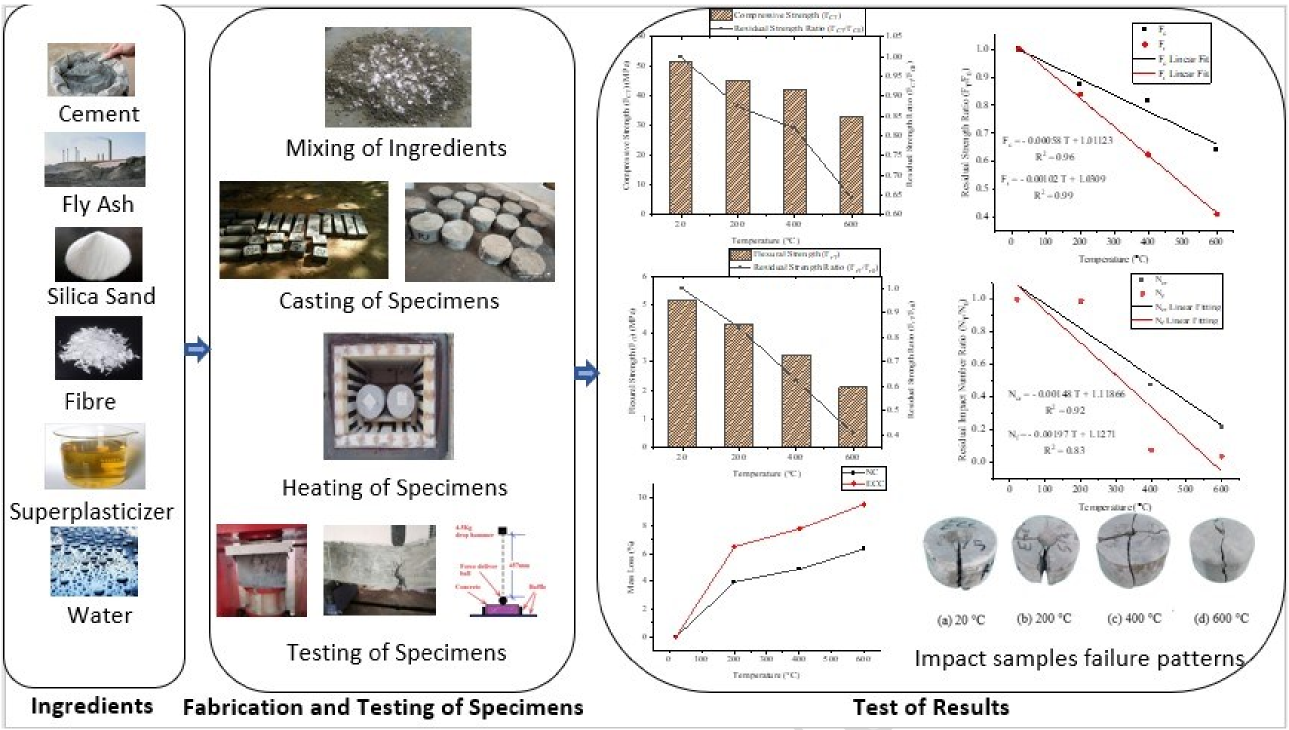

ABSTRACT

The study conducted a practical examination to evaluate the influence of high temperatures on the strength and repetitive impact performance of Polypropylene fiber-reinforced Engineered Cementitious Composites (ECCs). Compressive and bending strength were examined using cylindrical and beam-shaped specimens, respectively, while repetitive impact evaluations were conducted on cylindrical specimens following ACI 544-2R methodology. The control samples were evaluated at ambient temperature, while three additional sets underwent testing after exposure to 200 °C, 400 °C, and 600 °C, followed by cooling. The outcomes demonstrated that the reference ECC samples displayed superior resistance to failure impacts compared to standard concrete, characterized by a yielding catastrophe pattern. Despite a decline in impact resistance and ductility following exposure to temperatures of 200 °C, 400 °C, and 600 °C, ECCs still outperformed normal concrete. The number of impacts leading to failure decreased from 260 to 258, 20, and 10 specimens following exposure to temperatures of 200 °C, 400 °C, and 600 °C, respectively, maintaining ECCs' impact resistance at least four times greater than that of conventional concrete counterparts. This study also examined the durability of ECC and normal concrete, focusing on rapid chloride penetration, sorptivity, water absorption, acid attack, and sulphate attack. ECC demonstrated superior durability across all measures, attributed to its high tensile strain capacity and controlled micro-crack width.

Keywords: impact; elevated temperatures; ;Engineered Cementitious Composites; ; acid attack; sulphate attack; rapid chloride penetration; water absorption.

1. Overview

Irrespective of its intended function, any structural facility is susceptible to unforeseen and adverse loads. While recent reinforced concrete structures are constructed to endure distinctive gravity and lateral forces like wind and seismic forces, integrating accidental loading scenarios isn't a mandatory requirement in building design codes due to cost considerations. Accidental loads, whether from fires or impacts, pose significant risks, as fires can rapidly undermine load-bearing elements, and abrupt impacts have the potential to cause concentrated damage, posing a threat to overall structural integrity.

Despite advancements in fire-resistant systems and construction materials, the construction sector still experiences a significant number of fire incidents annually. In India, approximately 1.6 million fire accidents have been reported, while the UK has documented over 500,000 incidents, with structural fires constituting 40% of these occurrences (Arna'ot et al., 2017a; Brushlinsky et al., 2018). Globally, more than 100 million fire accidents have been recorded across 39 countries, resulting in over a million fatalities (Brushlinsky et al., 2018). Following a structural fire, a crucial decision must be made regarding the concrete structure's future whether it can resume normal occupancy, needs rehabilitation before reoccupation, or requires demolition (Albrektsson et al., 2011). This decision relies on a precise evaluation of concrete's enduring attributes, especially its mechanical strength in withstanding designated loads. The microstructure of concrete undergoes physical and chemical transformations influenced by the temperature reached during fire exposure and its duration, along with factors such as mix composition, porosity, and thermal features of aggregates (Albrektsson et al., 2011; Guo et al., 2014; Tufail et al., 2017; Babalola et al., 2021). As temperatures increase, various chemical and physical changes occur, impacting concrete strength due to its heterogeneous nature (Roufael et al., 2021). The evaporation of free water within the concrete is a primary consequence of fire at temperatures around 80°C to 120°C (Roufael et al., 2021; Drzymala et al., 2017, Abrams, 1971). More severe material degradation occurs at temperatures exceeding 300°C but remaining below 450°C, characterized by the removal of water from the C-S-H gel present in the hydrated cement matrix (Abrams, 1971; Dügenci and Haktanir, 2015; Arna'ot et al., 2017b; Chu et al., 2016). This phase is pivotal in the deterioration of concrete. Thermal influences induce varied reactions in the cement matrix and aggregate, causing bond separation at higher temperatures, contributing to the weakening of the concrete structure and a decline in its residual strength (Phan and Carino, 2003; Netinger et al., 2011; Deng et al., 2020; Phan and Carino, 1998; Roufael et al., 2021; Abrams, 1971). Tensile strength degrades at a quicker pace than compressive strength, and mechanical characteristics like bending strength, shear strength, and elasticity modulus also undergo considerable deterioration after exposure to temperatures around 500°C, as verified by numerous researchers (Al-Owaisy 2007; Sultan and Alyaseri, 2020; Cheng et al 2004; Husem 2006; Shallal and Al-Owaisy, 2007; Toric et al., 2013; Alimrani and Balazs, 2020).

In contrast, specific structural segments often endure accidental impact loads, like collisions with vehicles or falling objects, constituting instances of repeated accidental loads (Nili and Afroughsabet, 2010). For example, offshore structures face impacts from ocean waves, and hydraulic structures, like stilling basins, experience the force of water impacting the downstream runway. Additionally, airport runways encounter repeated impacts from airplane wheels (Salaimanimagudam et al., 2020; Wang and Chouw, 2017; Abid et al., 2020a). While various methods exist for assessing concrete's impact resistance, ACI 544-2R stands out, particularly for replicating conditions involving repeated impacts in the evaluation of Fiber Reinforced Concrete (FRC) characteristics.

In recent years, numerous research studies have delved into evaluating the repeated impact resistance of different concrete varieties using the ACI 544-2R testing methodology. Mastali et al. (2016) focused on the impact of the quantity and length of recycled carbon fiber-reinforced polymer on Self-Compacting Concrete (SCC). Ismail and Hassan (2017) explored the impact resistance of SCC mixes containing varying concentrations of Silica Fume (SF) and crumb rubber, noting a substantial improvement in impact ductility with the addition of crumb rubber and 1% SF. Mahakavi and Chithra (2019) investigated the effects of hooked-end and crimped SF on SCC, finding significant improvement when both fiber types were combined. Jabir et al. (2020) studied the impact resistance of ultra-high-performance concrete with micro-steel fibers and polypropylene (PP) fibers. Abid et al. (2020b; 2021a, b) conducted tests on SCC incorporating micro steel fibers, revealing that 1.0% SF led to an over 800% improvement in impact resistance compared to plain reference specimens. Murali et al. (2019; 2020; 2021a, b, c) and others (Ramkumar et al., 2019; Prasad and Murali, 2021; Ramakrishnan et al., 2021) explored repeated impact characteristics in fibrous concrete with multiple layers, demonstrating enhanced impact resistance during both cracking and failure phases with the inclusion of intermediate fibrous meshes, particularly steel fibers, showing the most significant enhancement in impact strength. These studies collectively contribute valuable insights into the impact performance of various concrete formulations, providing crucial information for applications where sustained repetitive impacts are a concern.

In contrast to conventional concrete with comparable fiber concentration and strength, ECCs emerge as high-performance variants of SCC, renowned for exceptional ductility, manifesting numerous cracks and strain hardening in response to tensile and flexural stresses. Li introduced ECCs in 1993, and since then, they have been widely utilized in various projects (Li 2007). Despite extensive research exploring diverse ECC formulations with varying fibers, studies specifically addressing the repeated impact behavior of ECCs are limited. Ismail et al. (2019) performed investigational investigations following the ACI 544-2R methodology, revealing significant impact performance improvement (15% to 20%) by incorporating fly ash and metakaolin into ECCs. Existing literature also includes studies on the behavior and residual mechanical characteristics of various ECC mixes after exposure to fire (Sahmaran et al., 2010; Çavdar, 2012; Shang and Lu, 2014; Rafiei et al., 2021). The examination of existing literature reveals a notable scarcity of experimental studies focusing on enduring ECC’s repetitive impact strength. Moreover, there exists a notable knowledge gap regarding the sustained impact resistance of Fiber-Reinforced Concrete (FRC) under elevated temperatures. To the authors' knowledge, there is no prior research that has explored the enduring repetitive impact strength of ECCs following exposure to elevated temperatures, specifically reaching up to 600 °C. To fill this gap, this study seeks to expand upon existing knowledge by investigating the influence of high temperatures on the mechanical and durability properties of ECCs. The scope of this research includes a comprehensive evaluation of ECCs under both ambient and elevated temperature conditions. The primary objectives are to assess the changes in compressive, bending, and repetitive impact strength, and ductility performance of ECCs after exposure to temperatures of 200 °C, 400 °C, and 600 °C. This evaluation is critical as real-world applications often subject concrete structures to extreme thermal conditions, which can significantly affect their structural integrity and lifespan. The comparison between ECC and conventional concrete in this study aims to highlight the enhanced properties of ECC, such as improved ductility, superior crack control, and greater durability. These performance improvements are directly attributable to the optimized mix design of ECC, which includes a higher water-to-cement ratio, the inclusion of supplementary cementitious materials (SCMs), and the use of fibers. Therefore, the performance-based comparison is both relevant and necessary to demonstrate the advantages of ECC in specific engineering applications. Moreover, the study aims to compare the durability of ECCs and normal concrete through various tests including rapid chloride penetration, sorptivity, water absorption, acid attack, and sulphate attack. By doing so, the research seeks to establish ECCs' superiority over normal concrete in terms of resistance to environmental and chemical degradation. The outcomes of these tests are expected to provide valuable insights into the practical applications of ECCs in constructing more durable and resilient infrastructure.

2. Environmental Impacts of Waste Management and ECC Benefits - Background

The environmental impact of waste management practices is a critical concern in modern society, as traditional methods often lead to significant ecological degradation and resource depletion. Concrete production, a major contributor to construction waste, consumes vast amounts of natural resources and energy while generating substantial carbon emissions. Furthermore, the disposal of concrete waste adds to the burden of landfills, exacerbating environmental pollution and habitat destruction. In this context, the adoption of innovative materials like Polypropylene fiber-reinforced Engineered Cementitious Composites (ECCs) holds considerable promise for mitigating the environmental footprint of waste management practices. ECCs offer several distinct advantages over conventional concrete, including enhanced durability, crack resistance, and resilience to harsh environmental conditions. These properties are particularly beneficial in the context of waste management infrastructure, where structures are subjected to continuous stress and exposure to corrosive agents. By incorporating ECCs into waste management facilities, such as landfills, transfer stations, and recycling plants, several environmental benefits can be realized. Firstly, the superior durability of ECCs ensures longer service life and reduced maintenance requirements, leading to decreased material consumption and waste generation over time. Additionally, ECCs' resistance to chemical attack and environmental degradation minimizes the need for protective coatings and repair interventions, further reducing resource consumption and environmental impact. Moreover, the use of ECCs in waste management infrastructure can facilitate the construction of more robust and resilient facilities capable of withstanding the challenges posed by waste handling and disposal processes. This increased durability not only enhances the operational efficiency and safety of such facilities but also reduces the risk of environmental contamination and groundwater pollution due to structural failures.

3. Materials and Approaches

3.1. Concrete Blends and Constituents

This study aims to assess the sustained impact resilience of ECCs following exposure to elevated temperatures. ECCs, a contemporary concrete type, have no presence of coarse aggregate and feature a substantial concentration of fine cementitious and filler components. This investigation employs the established M45 ECC mix, known for its recognized characteristics (Li 1993; Li 2007). In this research, the M45 formulation is adjusted by introducing Polypropylene (PP) fiber as a cost-effective alternative to Polyvinyl Alcohol Fiber (PVA), as shown in Figure 1. For comparison, a conventional concrete mix with normal strength (NC), exhibiting a similar compressive strength, is included. Detailed mix proportions for both formulations are shown in Table 1.

Table 1. Quantities of materials in NC and ECC mixes (kg/m^3).

Mixture	Cement	Fly Ash	Sand	Silica Sand	Gravel	Water	SP	Fiber
ECC	570	700	-	460	-	320	5.0	18.6 (2% PP)
NC	420	-	802	-	858	210	-	-

Figure 1. Polypropylene Fiber used in this study

Ultratech's Ordinary Portland cement (Grade 53) was used in both mixes, with fly ash as an additional cementitious component exclusively in the ECC mix. Table 2 provides the physical characteristics and chemical composition of the fly ash and cement. The ECC formulation omitted sand and gravel, utilizing silica sand (particle size: 100 to 260 µm, bulk density: 1470 kg/m^3). The NC mix included local M-Sand as fine aggregate and crushed gravel as coarse aggregates from Madurai, Tamil Nadu, with particle grading details in Table 3 and a maximum gravel size of 20 mm. To ensure workability, the ECC mix employed BASF-Master Glenium Sky 8233, which is a superplasticizer based on polycarboxylic ether, complying with IS 9103-1999. Additionally, 2% by volume of Polypropylene (PP) fiber, detailed in Table 4, was incorporated into the ECC mix.

Table 2. Cement and fly ash characteristics.

Percentage of Oxide	Cement	Fly Ash
SiO_2	20.07	52.11
Fe_2O_3	4.62	7.39
Al_2O_3	5.32	23.59
CaO	61.85	2.61
MgO	0.83	0.78
SO_3	2.50	0.49
Specific surface (m^2/kg)	390	320
Specific gravity	3.13	2.26
Percentage of material retained in a 45 µm sieve	-	34%

Table 3. Particle size distribution of sand and gravel in Normal Concrete

Sieve Size (mm)	% Passing of Sand	% Passing of Gravel
20	100	89.2
12.5	100	65.2
10	100	5.5
4.75	100	1.1
2.36	95.5	0
1.18	81.4	0
0.6	69.9	0
0.3	37.5	0
0.15	33.4	0
0.075	16.2	0
Pan	0.5	0

Table 4. Characteristics of PP fibers.

Density in g/m^3	Length in mm	Diameter in microns	Tensile Strength in MPa	Melting Point in °C
0.89-0.94	12	35-40	350	162-167

3.2. Experimental Work Plan and Heating Procedure

For each concrete mix and across various temperature conditions, six disk samples with a diameter of 150 mm and a thickness of 64 mm underwent repeated impact tests following the drop weight released freely method outlined in ACI 544-2R. Additionally, a set of six-cylinder specimens, each measuring 100 mm in diameter and 200 mm in height, were utilized for a compressive strength test following IS:516:1959 standards as illustrated in Figure 2a. Furthermore, six beam specimens with a cross-section of 100 x 100 mm and a length of 500 mm underwent a four-point bending test for evaluating flexural strength, adhering to IS:516:1959 standards as illustrated in Figure 2b. All disk, cylinder, and beam samples were consistently subjected to curing under temperature-controlled water tanks for 28 days. Following the completion of the curing phase, the samples underwent a 24-hour drying process in the laboratory, considering previous research indicating potential explosive failure if initial drying is omitted. As a precaution, all specimens underwent pre-drying in an electric oven set at approximately 105 °C for 24 hours. Subsequently, a gradual heating process was applied using the electric furnace portrayed in Figure 3a, with a consistent amount of about four degrees Celsius per minute. This process achieved three distinct high-temperature thresholds: 200 °C to 600 °C with increments of 200 °C, maintaining each temperature level for 60 min to ensure thermal saturation. After opening the furnace door, samples were gradually cooled to reach room temperature before testing. Figure 3b illustrates the heating schedule for all temperature levels used. Additionally, a fourth set of specimens underwent testing at ambient temperature, as a reference one.

(a) Compressive Strength Test (b) Flexure Strength Test

Figure 2. Testing of Specimens

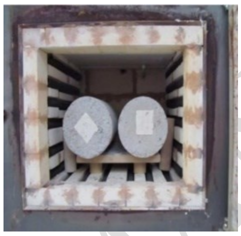

(a) Electrical furnace

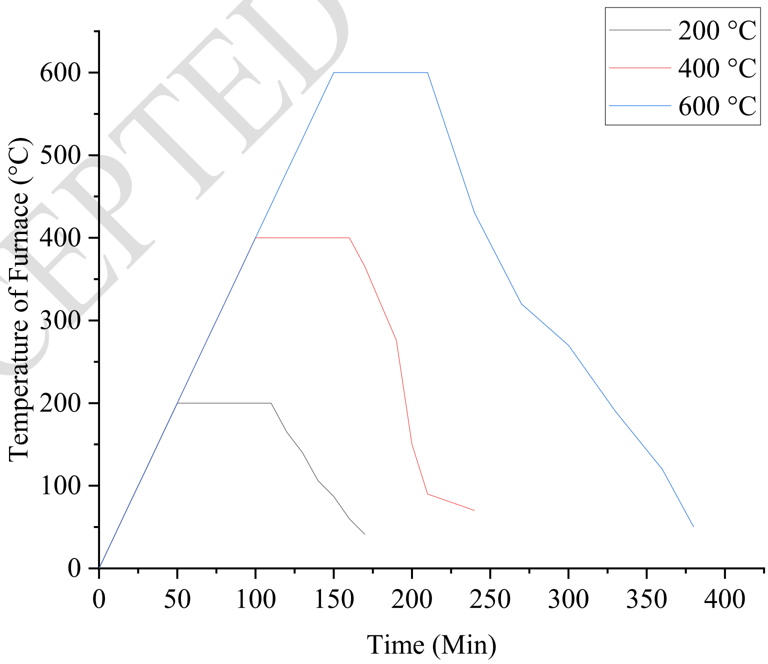

(b) Temperature profile during heating

Figure 3. Heating process of the test samples

3.3. Evaluation of Repetitive Impact using Drop Weight

The evaluation of material and structural responses to impact often uses various testing methods, including the drop-weight test specified in ACI 544-2R. This standard describes two types of drop-weight tests. The primary type is the instrumented drop-weight test, which is typically used to assess the impact response of structural elements like reinforced beams and slabs, involving expensive sensors and advanced data acquisition systems. The alternative is a simpler drop-weight impact test conducted on smaller specimens without requiring instrumentation. In this test, a 4.54 kg weight is repeatedly dropped from a height of 457 mm onto the specimen until a visible surface crack appears, continuing until the specimen fractures. The cracking impact number and failure impact number represent the impacts at which the first crack and failure occur, respectively. This qualitative method allows for comparing the impact resistance of different concrete mixes by evaluating their ability to withstand impacts that cause cracking and failure. The typical test specimen is a cylindrical disk with a 150 mm diameter and 64 mm thickness. The test is performed manually by raising the drop weight to a specific height and releasing it to fall onto a steel ball positioned centrally on the sample's top surface. The steel ball, which helps distribute the load, is securely held in place by a specialized frame, as illustrated in Figure 4.

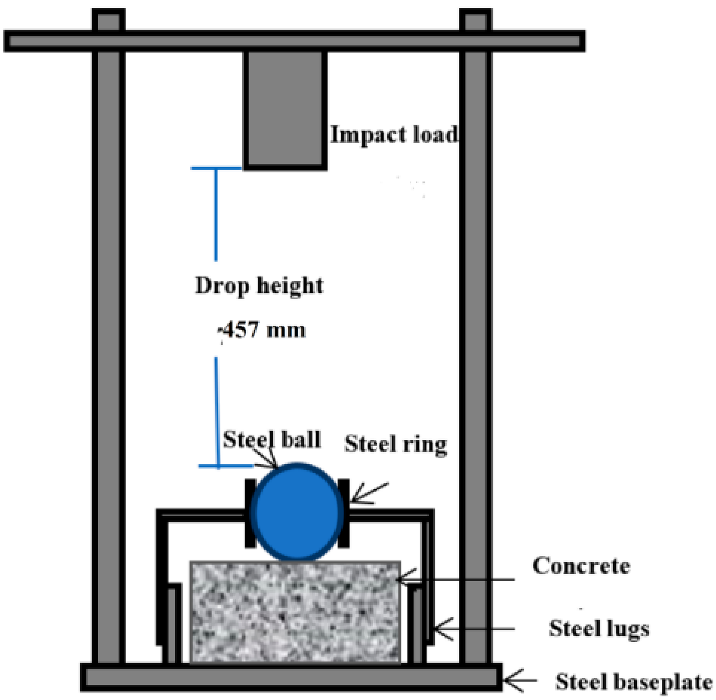

Figure 4. Schematic diagram of drop-weight impact test setup

3.4. Evaluation of Concrete's Durability Characteristics Test

3.4.1 Sulphate attack test

Cube specimens, 100mm x 100mm x 100mm, cured for 28 days, underwent a sulphate attack test. Immersed in 5% sodium sulphate solution at 23 ± 2°C for 90 days, they were monitored for surface cracks, as shown in Figure 5. Residual compressive strength and weight loss due to sulphate attack were assessed at intervals of 30, 60, and 90 days. Tests were conducted on three specimens per mix, with average values recorded.

3.4.2 Acid attack test

Cube specimens (100mm on each side) were water-cured for 28 days and then tested for acid attack. They were immersed in a 1% sulphuric acid solution at 23 ± 2°C for 90 days and monitored for surface cracks or damage, as shown in Figure 5. Residual compressive strength and weight loss were measured at 30, 60, and 90 days. Compression strength tests were performed on three specimens per mix, with the average values recorded. This process evaluated the concrete's durability against acid attack over time, providing insight into the material's long-term performance under these conditions.

3.4.3 Water Absorption Test

Water absorption tests were performed on 100mm cube specimens after 28 days of curing, following ASTM C 642. The water-saturated specimens were weighed, dried in a hot air oven at 105°C (Figure 6), then cooled and reweighed. The difference in weight between the water-saturated and oven-dried specimens determined the water absorption value. This process will provide an accurate measure of each mix's water absorption capacity.

Figure 5. Sulphate and Acid attack test

Figure 6. Water Absorption test

3.4.4 Sorptivity Test

The sorptivity test, following ASTM C 1585, measures water absorption by capillary action on homogeneous material. After 28 days of curing, 100mm cube specimens were oven-dried at 100 ± 10°C, as shown in Figure 7. They were then placed in a tray with a water level 5mm above the base, with peripheral surfaces sealed with a non-absorbent coating. The water absorbed was measured over 30 minutes by weighing the specimens after wiping off excess water. The cumulative water absorption increased with the square root of the elapsed time.

$$\text{Sorptivity, } S = I/\sqrt{t}$$

$$I = (W_2 - W_1) / A \times d$$

Where, t = Elapsed time in minutes.

W_1 = Oven dry weight of specimen in grams

W_2 = Weight of specimen after 30 minutes of capillary suction of water in grams

A = Surface area of the specimen through which water penetrated in mm^2

d = Density of water in g/mm^3

3.4.5 Rapid Chloride Permeability Testing (RCPT)

The resistance of mixtures to chloride ion penetration was assessed using RCPT following ASTM C1202 guidelines. For each mix, three-disc specimens, each 50mm thick and 100mm in diameter, underwent testing, and the average RCPT value was determined. Applying a 60V DC for 6 hours, one end of the specimens was immersed in a 3% Sodium Chloride solution while the other end was placed in a 0.3M Sodium Hydroxide solution, as shown in Figure 8.

Figure 7. Sorptivity test

Figure 8. Rapid Chloride Permeability Test

4. Outcomes from Standard Experiments

4.1. Compressive Strength

Figure 9 illustrates the relationship between temperature and residual compressive strength in ECC cylinders, while Figure 10 presents the corresponding data for Normal Concrete (NC) specimens. In Figure 9, ECC's compressive strength decreases by about 13% at 200 °C, from the initial 51.7 MPa to 45.2 MPa. Subsequent exposure to 400 °C results in a more modest decline, with residual strengths of approximately 87% and 82% at 200 °C and 400 °C, respectively. At 600 °C, ECC experiences a notable strength decrease, reaching 33.2 MPa, reflecting a 36% loss compared to unheated specimens. In contrast, NC exhibits a smaller strength reduction following exposure to temperatures of 200°C and 400°C, residual strengths were observed around 92% at both temperatures, as depicted in Figure 10. However, at 600 °C, both NC and ECC demonstrate a similar residual compressive strength ratio of approximately 35% less as compared to unheated specimens.

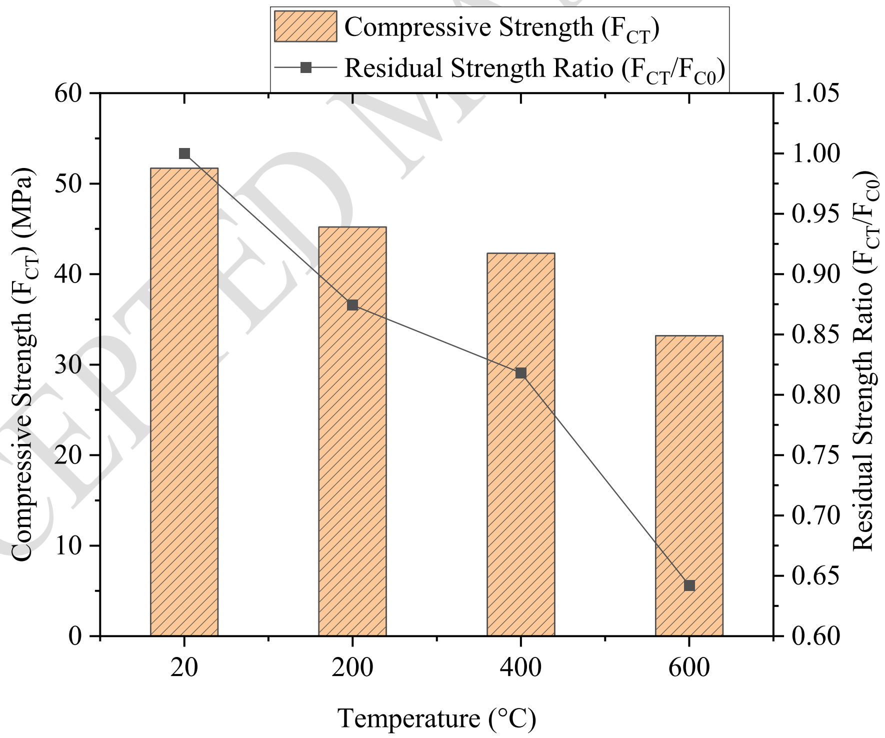

Figure 9. Compressive strength remaining in ECC under diverse temperature conditions

The more significant reduction in strength observed in ECCs between 200 °C and 400 °C can be attributed primarily to their denser microstructure compared to NC. ECCs, characterized by a higher proportion of binder and silica sand, excluding coarse aggregate, result in reduced water/binder content and lower porosity than NC. Heating below 200°C causes the evaporation of free pore water, leading to the buildup of pore pressure within the microstructure. In NC specimens, higher porosity facilitates pressure dissipation, relieving internal thermal stresses. However, in ECC, with its denser microstructure, higher stresses lead to considerable reductions of strength in compression experiential at 200 °C and 400 °C. Previous research (Sahmaran et al., 2011) documented ECC's decrease in the volume of pores, including those larger than 0.1 μm, following exposure to 400 °C. This decrease is related to the pozzolanic reaction, which includes other cementitious materials and unhydrated fly ash, leading to undesirable volume changes, additional formation of C-S-H gel, microstructural cracks, and a subsequent decline in strength. The significant strength decreases at 600 °C result primarily from the dehydration of hydrated products beyond 400 °C, causing microstructural degradation with an increase in pore number and size, along with alterations in volume causing microscopic crack formation. Sahmaran et al. (2010) noted a considerable rise in both pore volume and size in ECC after exposure to 600 °C, resulting in a 9% porosity increase, significantly different from the 5% rise observed following exposure to 400 °C. Furthermore, the size of the pore expanded by 300% after exposure to 400 °C.

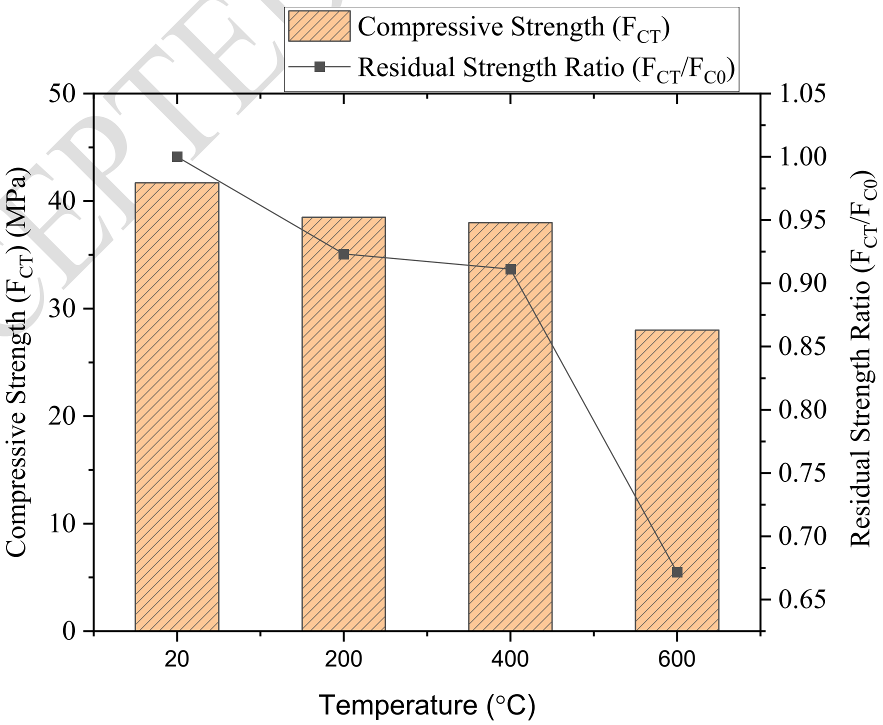

Figure 10. Compressive strength remaining in NC under diverse temperature conditions.

4.2. Flexural Strength

Figure 11 depicts the progressive reduction in the flexural strength of Engineered Cementitious Composites (ECC) with increasing temperature, extending up to 600 °C. Initially, at room temperature, ECC exhibited a flexural strength of 5.17 MPa. This value diminished to 4.34 MPa, 3.23 MPa, and 2.12 MPa following exposure to temperatures of 200 °C, 400 °C, and 600 °C, respectively. These reductions in strength amounted to approximately 16%, 38%, and 59% at the respective elevated temperatures. Likewise, Figure 12 illustrates a consistent and substantial decline in the flexural strength of Normal Concrete (NC) as the temperature ascends. At temperatures reaching 200 °C, 400 °C, and 600 °C, the flexural strengths of NC samples measured 2.95 MPa, 2.15 MPa, and 0.75 MPa, respectively, in contrast to the control specimens, which were not subjected to heating, and showed a 3.67 MPa as flexural strength. Consequently, the proportion decreases amounted to around 20%, 41%, and 80% at temperatures of 200 °C, 400 °C, and 600 °C, correspondingly.

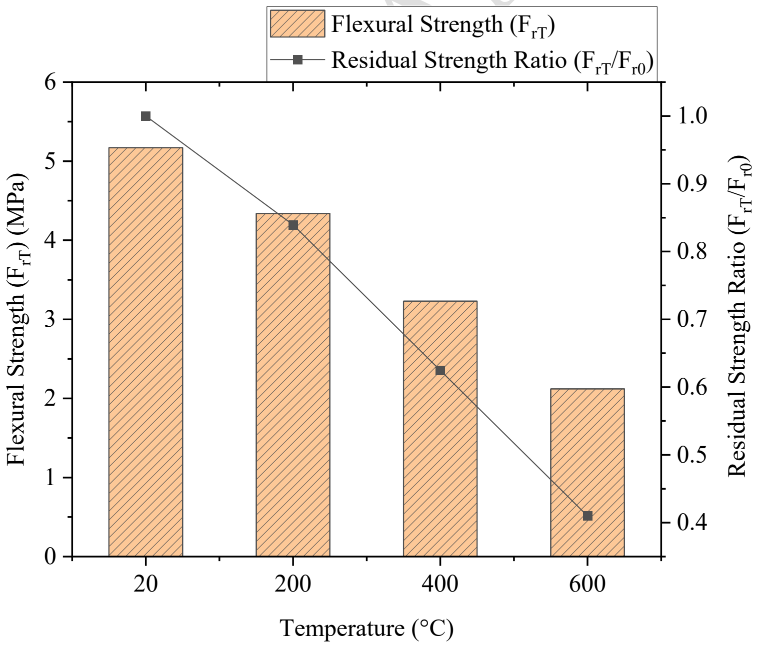

Figure 11. Flexural strength remaining in ECC at various temperature exposures

The gradual decline in flexural strength noted following exposure to high temperatures is often linked to changes in the volume of the cement matrix induced by vapor movements surpassing 100 °C. Moreover, the weakening of the connection between the filler and binder becomes more pronounced after reaching 400 °C owing to their unique thermal characteristics. Chemical reactions, including the drying out of C-S-H and increased porosity, significantly contribute to degradation, particularly beyond 400 °C. While the initial higher flexural strength of Engineered Cementitious Composites (ECC) is associated with the crack-bridging activity of Polypropylene (PP) fibers and a higher proportion of cementitious materials, this bridging effect diminishes exceeding 200 °C as a result of PP fibers melting. ECC shows superior performance at increased temperatures relative to NC, is due to the smaller particles and no presence of coarse aggregate, minimizing the adverse effects of bond weakening. Studies by Wang et al. (2021) and Zhihui et al. (2020) align with our findings, indicating substantial residual flexural strength in ECC after exposure to elevated temperatures, showcasing its resilience.

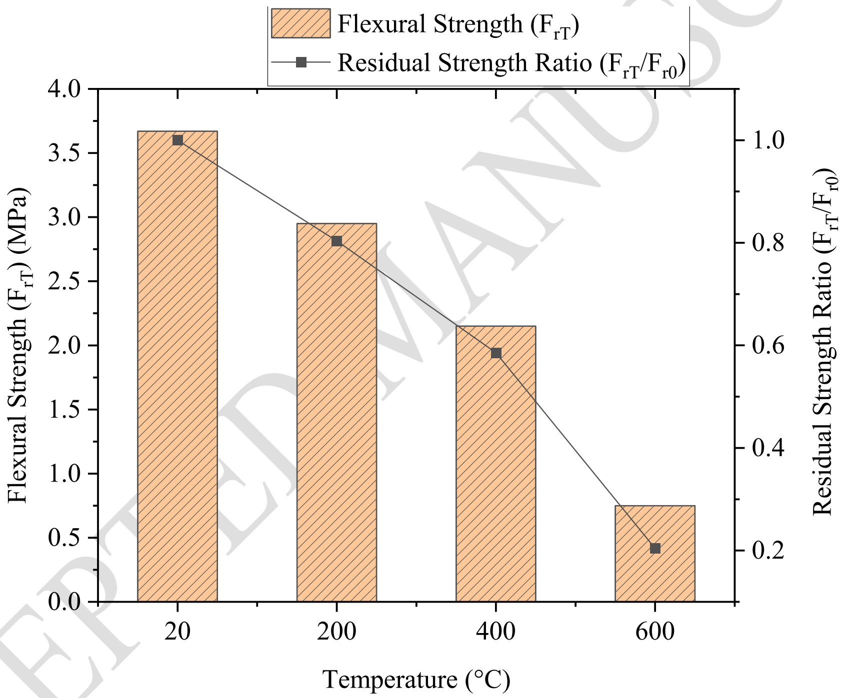

Figure 12. Flexural strength remaining in NC at various temperature exposures

4.3 Effect of Elevated Temperatures on Mass Loss

Illustrated in Figure 13 is the mass loss observed in various types of concrete when subjected to elevated temperatures. The decrease in mass is a consequence of the evaporation of unbounded water at initial stages and bound water between 150°C and 300°C, converting into water vapor at higher temperatures. In NC, a mass loss of 4.90% at 400°C was primarily due to water evaporation. Between 400°C and 600°C, a relatively smaller variation in mass (6.34%) indicated significant prior water evaporation, influenced by cracking at 600°C, releasing dehydrated sand, slag, and cement paste. ECC, with low permeability, was expected to have lower mass loss than NC up to 200°C. However, ECC exhibited higher mass loss at both 200°C (6.51%) and 400°C (7.78%) compared to NC, as a result of PP fibers melting at 200°C. By 400°C, melted fibers contributed to the mass decrease, reducing PP fibers' content in the concrete. The melting of PP fibers also created pores, allowing water vapor to escape. Despite ECC's low permeability, this mechanism prevented explosive spalling. Similar to NC, cracks in ECC between 400°C and 600°C released small amounts of dehydrated components during cracking.

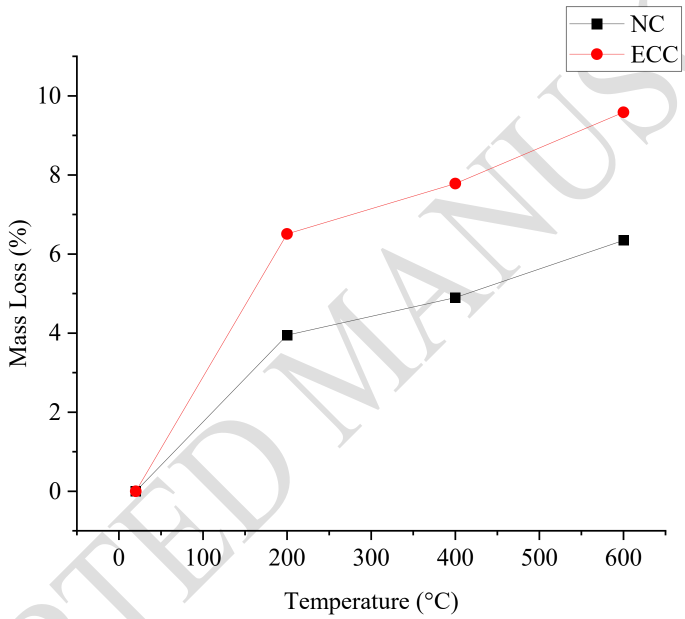

Figure 13. Mass loss in all concrete types after heating

5. Outcomes of Repeated Impact Testing

5.1. Details of Heated Test Samples

The data presented in Figure 14 outlines the external surface characteristics of a baseline impact disk sample and additional samples subjected to pre-testing heating at temperatures of 200 °C, 400 °C, and 600 °C. Visual inspection revealed there were no notable changes in the appearance of the specimens following exposure to high temperatures. Nevertheless, a noticeable lightening of the grey color was noted at 200 °C, and specimens exposed to 600 °C displayed small yellow areas. This subtle color change is likely linked to the breakdown of C-S-H gel particles, as noted in previous research

(Li et al., 2016; Liu et al., 2018; Li et al., 2019). It's worth noting that Polypropylene (PP) fibers lose their resilience at high temperatures due to their melting point being below 200 degrees Celsius. The inclusion of PP fibers played a crucial role in connecting crack surfaces, resulting in a slower and more ductile failure in the untreated reference specimens, as depicted in Figure 15a. However, exposure to temperatures of 400 °C and above resulted in the complete melting of fibers, eliminating the bridging effect and creating a more porous medium. The channels created upon fiber melting interconnected, establishing continuous porous networks that contributed positively to relieving internal stresses through vapor pressure dissipation. However, these channels could potentially have a detrimental effect by increasing the porosity of the material, which may render it more susceptible to brittleness under loads. Figure 15b illustrates that exposure to 600 °C led to the vaporization of PP fibers, causing an internal color change to dark gray and leaving behind a highly porous structure.

(a) 20 °C (b) 200 °C (c) 400 °C (d) 600 °C

Figure 14. Impact testing samples exposed to varying temperatures

(a) 20 °C (b) 600 °C

Figure 15. Visual representation of PP fibers in impact specimens before and after heat exposure

5.2 Numbers of Cracking and Failure Impacts

Figure 16 illustrates the cracking numbers (N_{cr}) observed in NC and ECC at various elevated temperatures, while Figure 17 displays the failure numbers (N_f). It's important to note the recognized variability in outcomes of the ACI 542-2R test. Specifically, the Coefficient of Variation (COV) for N_{cr} measurements in ECC ranges from 38% to 62.6%, and for N_f outcomes, it extends from 30.9% to 61.8%. Before exposure to elevated temperatures, Normal Concrete exhibits a higher initial cracking number compared to Engineered Cementitious Composites, primarily due to the presence of gravel, enabling NC to endure more impacts before cracking. However, after exposure to high temperatures, NC samples display a significantly weaker response and degrade more rapidly than their ECC counterparts. This can be attributed to the fundamental differences in material composition and stress distribution mechanisms. The fibers in ECC provide superior crack-bridging capabilities, leading to controlled microcracking and fewer visible cracks. In contrast, NC, while benefiting from the compressive strength contributed by gravel, experiences higher stress concentrations at the aggregate-matrix interface. These stress concentrations result in the initiation and propagation of more cracks under the same loading conditions compared to ECC. Specifically, the unheated cracking numbers (N_{cr}) were 42 for ECC and 57 for NC, each being the average of six recorded specimens. In contrast, following temperatures of 200 °C to 600 °C at 200 °C intervals, the remaining ECC cracking counts were forty-one, twenty, and nine, correspondingly, while the respective values for NC samples were fifteen, four, and two when subjected to identical levels of temperatures.

The results demonstrate a significant decline in cracking impact numbers for NC, with remaining values of Ncr dropping to just 25.8%, 5.5%, and 1.8%, correspondingly, relative to the unaffected baseline specimens, as depicted in Figure 16b. In contrast, ECC experienced a minor decrease of below 5% following exposure to 200 °C, whereas the remaining values of N_{cr} decreased to 45% and 20.4% following exposure to four hundred and six hundred degrees Celsius. The notable reduction in NC's N_{cr} is attributed to observed physical and chemical changes at elevated temperatures, including the dehydration of C-S-H and shifts in cement paste and aggregate. This makes the internal structure more brittle at higher temperatures, leading to rapid cracking. ECC, characterized by a finer matrix, greater amount of binder, and no presence of coarse aggregate, proves more resilient, enduring more impacts before cracking. Despite PP fibers having a melting point below 200 °C, a significant quantity persists at 200 °C, playing a crucial role in maintaining a substantial impact number before cracking, nearly equivalent to unheated specimens (95.8%). This resilience aligns with Aslani and Wang's

(2019) findings that PVA fibers retained structural integrity even after exposure to temperatures as high as 300 °C, exceeding the anticipated melting range of PVA, which is from 200 to 230 °C.

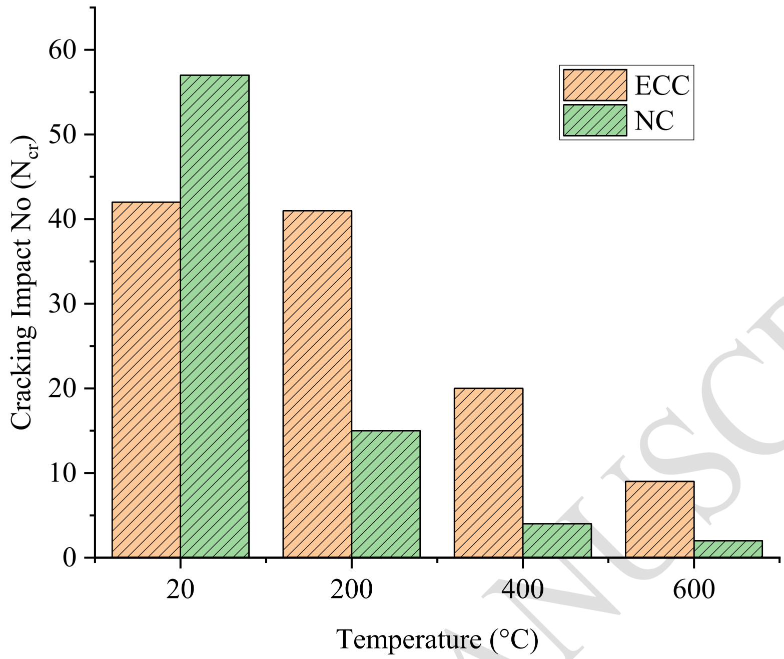

(**a**) Cracking number

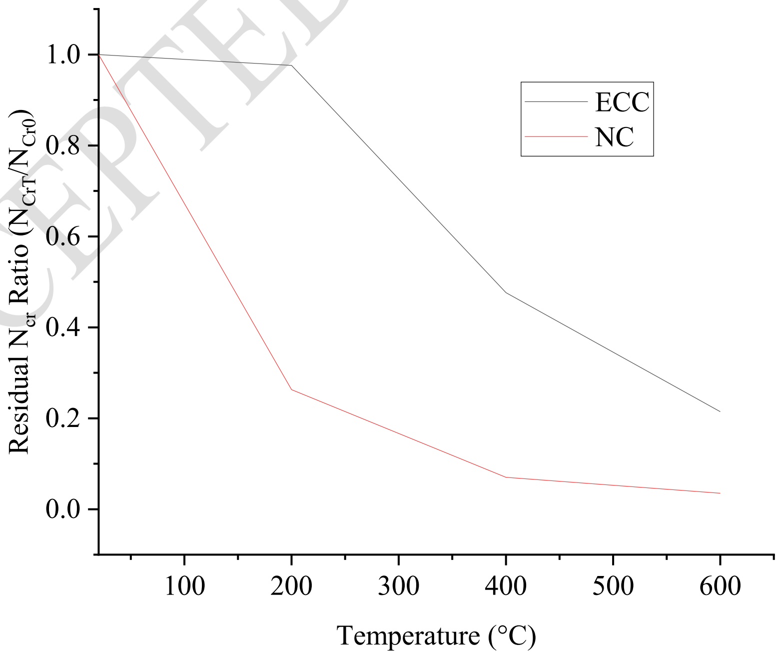

(b) Ratio of remaining cracking numbers.

Figure 16. Cracking impact numbers that persist in ECC and NC under different temperatures

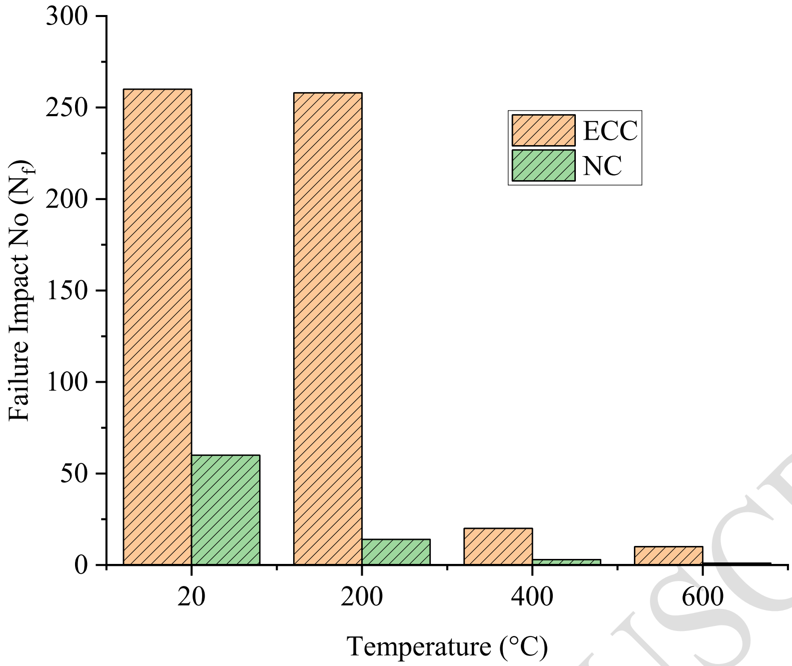

(**a**) Failure number

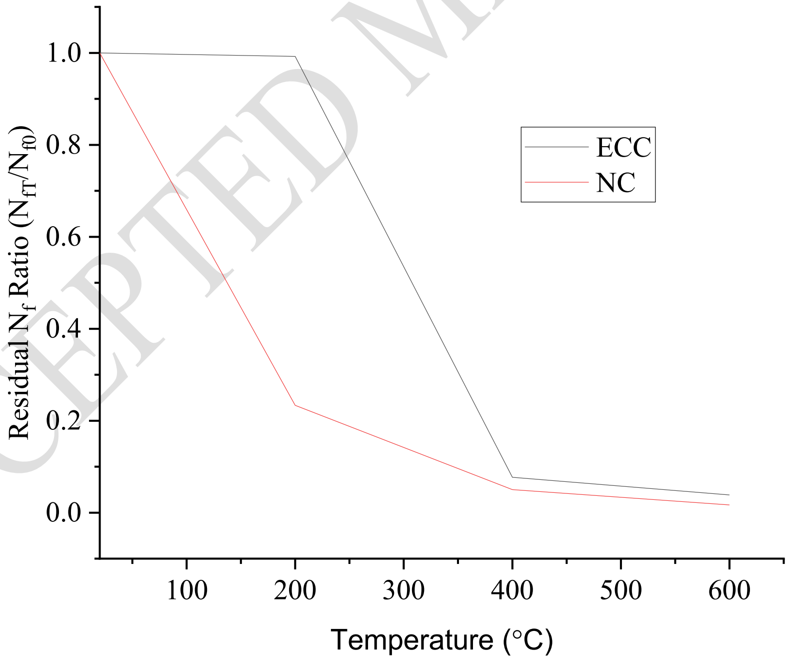

(**b**) Ratio of remaining failure numbers

Figure 17. Remaining impact values for ECC and NC at various temperature levels

Engineered Cementitious Composites are widely recognized for their exceptional capacity to undergo plastic deformation following cracking under both flexural and tensile loads. This resilience stems from their distinctive microstructure, featuring a high concentration of fine filler and binder, along with the fibers' ability to withstand increased tensile forces along cracks. These attributes not only enable ECC samples to absorb a considerably greater amount of energy than NC after experiencing cracks but also demonstrate this ability under repeated impact loads. Figure 17 illustrates that the number of impacts leading to failure (N_f) for ECC samples not subjected to heating exhibits a notable increase related to its respective N_{cr}, whereas NC's N_f closely aligns with its cracking number. Consequently, there is a considerable disparity in N_f between ECC and NC, despite NC having a higher N_{cr} than ECC. Unheated ECC shows an N_f of 260, surpassing NC's Nf of 60 by a significant margin. This indicates that NC's N_f is nearly identical to its N_{cr}, with just 3 additional impacts, while ECC endures 210 additional impacts following the occurrence of cracks.

After being subjected to a temperature of 200 °C, NC samples exhibited a significant decline, experiencing a reduction of about 73% in their preliminary performance under failure impacts, preserving just 15.2 impacts before reaching failure. In contrast, ECC samples maintained a relatively consistent failure strength compared to the unheated specimens, as discussed earlier. After undergoing a temperature of 200 °C, the residual N_f of ECC closely resembled the unheated N_f, amounting to 258 impacts. This suggests that the partial melting of polypropylene fibers at 200 °C and the hydration of unhydrated products may have contributed to this resilience. However, as temperatures exceeded 200 °C, the ECC microstructure deteriorated rapidly due to the thorough vaporization and melting of polypropylene fibers at approximately 340 °C, accompanied by the C-S-H gel decomposition (Poon et al., 2004). Consequently, the impact strength experienced a sharp decline following exposure to 400 °C and 600 °C. The remaining N_f percentages after being subjected to these temperatures were just 9.2 and 3.8, correspondingly.

5.3. Observed Failure Patterns in Impact Test Samples

The observations following failure in a standard ECC sample and those exposed to various elevated temperatures after repetitive impact loading are illustrated in Figure 18. In Figure 18a, the central loading region on the upper surface of the standard sample displays evident fracturing resulting from inflicted damage. This fractured area is a consequence of the steel ball applying repetitive concentrated compressive stresses, showcasing the material's capacity to absorb substantial impact energy under concentrated loading. Even when the surface layer fractures, PP fibers continue to bridge interior micro-cracks, resisting the attempt of compressive impacts to cause cylinder splitting and generating interior tensile stresses, as depicted in Figure 15a. Nevertheless, continuous impacts could eventually lead to fiber rupture or detachment from the surrounding material, causing gradual expansion and spread of cracks. Consequently, visible surface cracks emerge apparent. Figure 18a illustrates the ductile failure behavior of standard specimens, characterized by a central zone of fracture and multiple outward cracks.

(a) 20 °C (b) 200 °C (c) 400 °C (d) 600 °C

Figure 18. Patterns of failure witnessed in impact samples subjected to varying temperatures.

Following exposure to 200°C, ECC samples demonstrated failure patterns similar to unheated specimens, albeit with fewer standing fibers along the primary crack. However, minor cracks at this temperature were wider, indicating reduced ductility and increased brittleness compared to unheated samples (Figure 18b). Exposure to 400°C and 600°C caused significant damage to the ECC microstructure, leading to vaporization of reinforcing components, especially PP fibers. This resulted in brittle failure, characterized by breaking into 2, 3, or 4 fragments with wide cracks. Specimens weakened by higher temperatures showed reduced capacity to withstand substantial and concentrated impacts compared to reference and 200°C conditions, as depicted in Figures 18c and 18d.

6. Results on the Durability Properties of Concrete

6.1 Sulphate Attack

Table 5 illustrates the effects of sodium sulphate immersion on normal concrete and ECC. Figure 19 depicts the compressive strength of various concrete specimens after 30, 60, and 90 days of sulphate curing, and after 28 days of water curing. The weight loss in ECC is consistently lower than in regular concrete, as shown by the range of 1.61% to 3.17% compared to 2.12% to 4.1%. The lower weight loss in ECC indicates better durability and resistance to damage mechanisms that cause material loss. The reduction in compressive strength for ECC is consistently lower and less variable than that for regular concrete. The maximum strength reduction in ECC (24.61%) is significantly lower than the maximum strength reduction in regular concrete (31.48%). Fibers in ECC enhance denser and more durable, improving resistance to sulphate attack over normal concrete.

Table 5. Results of Sulphate Attack Test

Mix	Initial Weight (g)	% weight loss			Compressive strength after 28 days water curing	Compressive strength after sulphate attack		
		@ 30 days	@ 60 days	@ 90 days		@ 30 days	@ 60 days	@ 90 days
Control	1984	2.12	3.2	4.1	52.1	48.2	42.4	35.7
ECC	2021	1.61	2.64	3.17	64.6	61.2	54.3	48.7

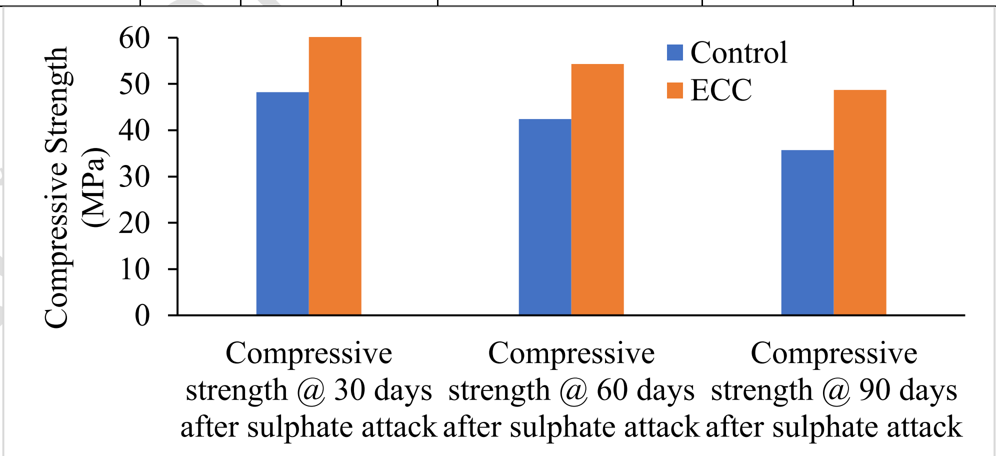

Figure 19. Results showing compressive strength after different ages of sulphate attack

6.2 Acid Attack

Table 6 and Figure 20 show the percentage of weight loss and compressive strength for normal concrete and ECC. The weight loss increased with longer curing periods. ECC exhibited less weight loss and higher compressive strength than normal concrete, indicating greater density and fewer pores. This demonstrates ECC's superior durability compared to normal concrete mixes.

Table 6. Results of Acid Attack Test

Mix	Initial Weight (g)	% weight loss			Compressive strength after 28 days water curing	Compressive strength after acid attack		
		@ 30 days	@ 60 days	@ 90 days		@ 30 days	@ 60 days	@ 90 days
Control	2044	2.53	3.26	4.54	52.1	46.1	40.7	33.4
ECC	2076	2.16	2.93	3.72	64.6	58.4	52.9	47.8

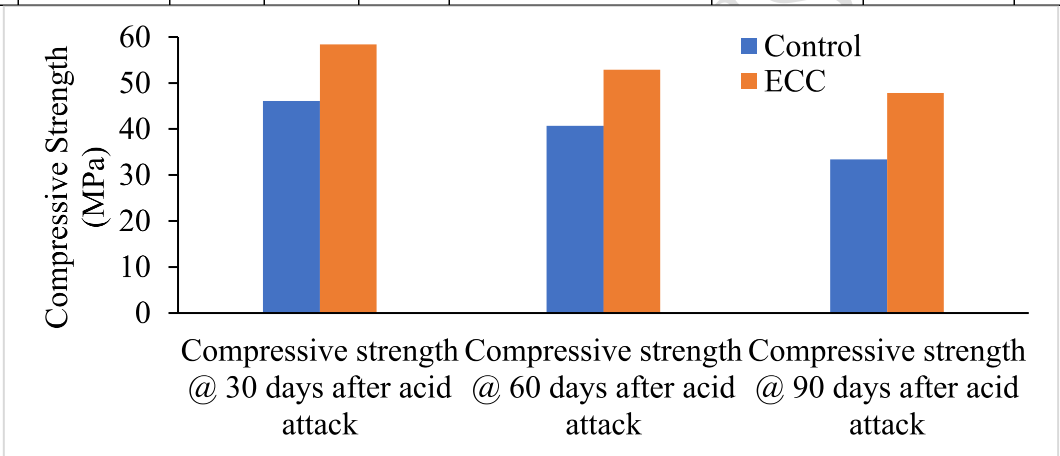

Figure 20. Results showing compressive strength after different ages of acid attack

6.3 Water absorption test

Table 7 shows the water absorption of normal concrete and ECC. Figure 21 illustrates the mix versus water absorption percentage. Normal concrete, lacking fibers, has higher permeability and water absorption compared to ECC, which demonstrates lower water absorption due to its fiber content.

Table 7. Water Absorption Test Results

Mix Name	Initial Weight (g)	24 Hours in oven (g)	Immersed in water (g)	% water absorption
Control	2032	2032	2212	8.86
ECC	2062	2072	2226	7.43

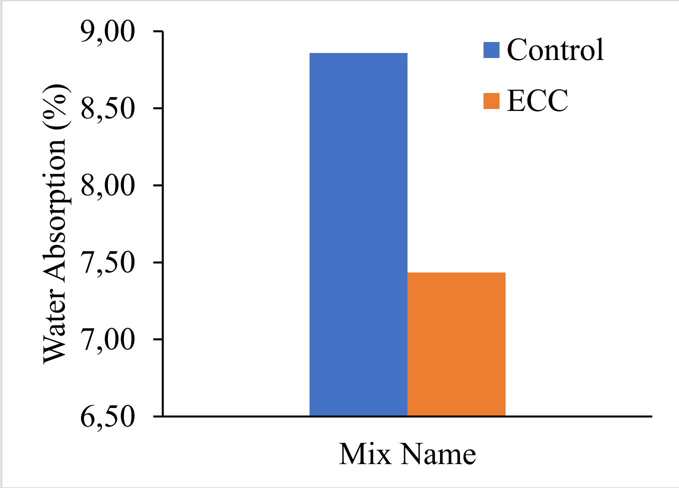

Figure 21. Results showing % of water absorption after 28 days of water curing

6.4 Sorptivity test

Table 8 shows that the sorptivity coefficient is lower for ECC compared to conventional concrete, as illustrated in Figure 22. The results indicate that normal concrete has more pores than ECC. ECC's refined, denser microstructure, achieved through fine fillers and higher cementitious content, limits water movement. Additionally, the use of Supplementary Cementitious Materials (SCMs) like fly ash or silica fume enhances the matrix, reducing water permeability. These factors collectively decrease ECC's sorptivity coefficient, indicating superior resistance to water absorption and greater durability compared to conventional concrete.

Table 8. Sorptivity Test Results

Mix	**Dry Weight (W_1) g**	**Wet weight (W_2) g**	**S = I/t½ (m/m$^{0.5}$)**
Control	2074	2104	0.00055
ECC	2109	2132	0.00042

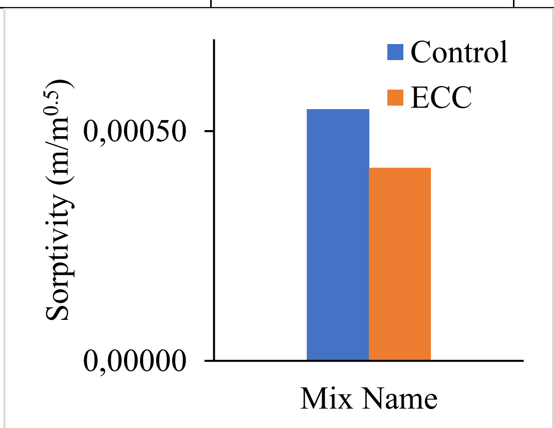

Figure 22. Variation of sorptivity with respect to different mixes

6.5 Rapid Chloride Permeability Test

Concrete permeability ratings were determined based on the charge passing through the specimens, as shown in Figure 23 and summarized in Table 9. ECC has higher permeability resistance compared to conventional concrete due to several key factors: fiber reinforcement, a dense microstructure, the use of SCMs, optimized mix design, and chemical admixtures.

Table 11. RCPT Test Results

Mix	Charge passed (Coulombs)	Chloride permeability
Control	812.5	Very low
ECC	767.3	Very low

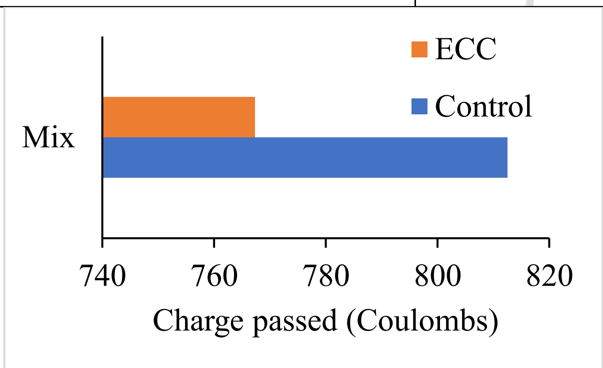

Figure 23. RCPT values of various concrete

7. Relationship Between Strength and Temperature

In specific scenarios, evaluating the sustained material strength following exposure to a particular temperature is crucial. When investigational information is limited, extrapolating from existing data for an initial assessment might be deemed acceptable. Figure 24 presents simplified correlations illustrating the correlation between the strength and impact values of ECC with added PP fibers post-elevated temperature exposure. It's essential to note the limited data points available for each fitting. Figure 24a shows that linear fits effectively capture the interaction between temperature and both compressive and flexural strength, achieving commendable determination coefficients (R^2) of 0.96 and 0.99, respectively. While Figure 24c suggests a relation involving multiple variables could well define the decrease in strength under compression by rising temperature, the 0.96 R^2 justifies accepting the simpler correlation linearly.

The connection between impact numbers and temperature exhibited a less robust linear association compared to compressive and bending resistance. Figure 24b shows that the linear links between temperature and N_{cr}, as well as N_f, tended to undervalue conserved impact numbers, especially at 200 °C, while overestimating them at 400 °C. These discrepancies influenced the accuracy of the linear correlation, particularly evident in N_f, where the R^2 value reached 0.83, the smallest among the acquired values. Addressing this, various nonlinear correlations were explored, identifying the exponential correlation as the most fitting with a coefficient of determination of 0.83, indicating robustness. Figure 24c illustrates the exponential relationships accurately predicting the decrease in N_f and N_{cr} after being subjected to the peak temperatures namely 400 °C and 600 °C. Nevertheless, it's crucial to note that these relationships substantially underrated the remaining impact values post-exposure to 200 °C.

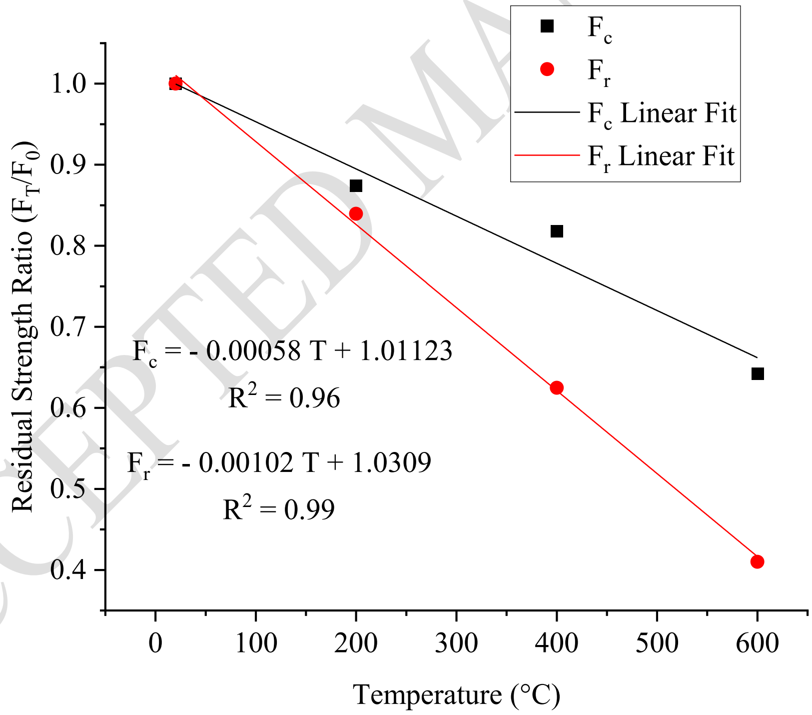

(a) Linear correlation related to strength

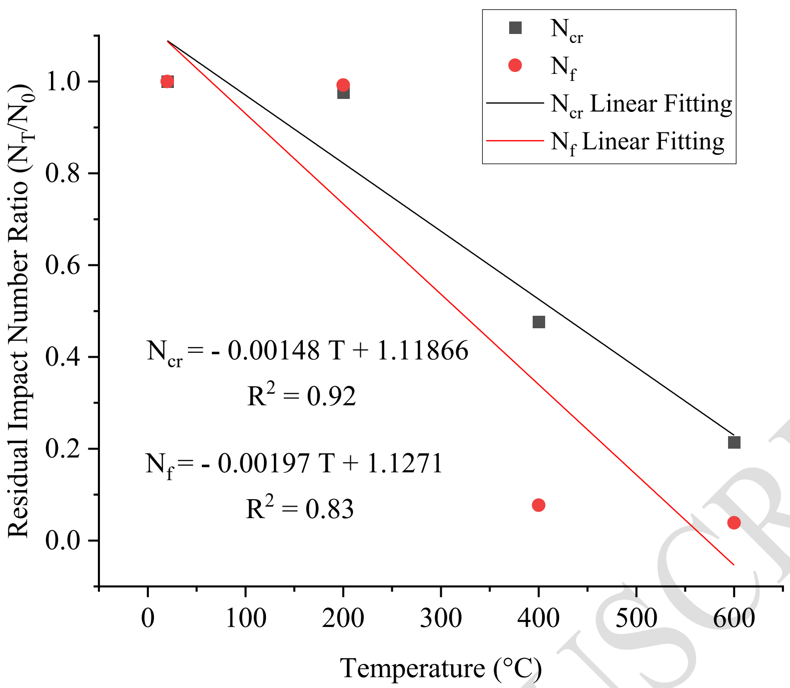

562

563 (b) Linear correlation concerning impact numbers

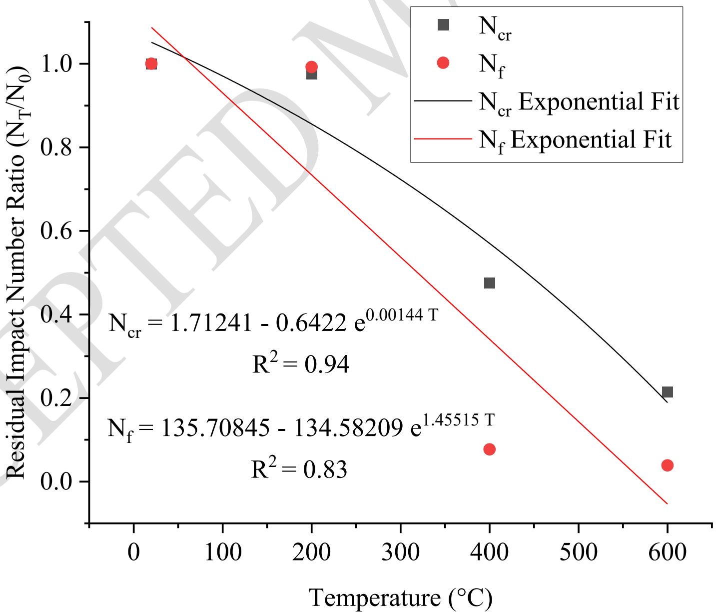

564

565 (c) Impact values Exponential correlation

566 **Figure 24.** Temperature correlation

567

568

8. Inferences

This study involved conducting compressive, flexural, and impact tests to assess the remaining strength of ECCs incorporating PP fibers after exposure to temperatures as high as 600 °C. The key conclusions drawn from the experimental findings in this research are as follows:

1. The ECC's compressive strength decreased with temperature rise, notably remaining constant at 200 °C and 400 °C but declining sharply at 600 °C. After exposure to 200 °C, 400 °C, and 600 °C, the residual compressive strengths were around 87%, 82%, and 64%, respectively. The reduction at 400°C is ascribed to chemical and physical alterations in the microstructure, including C-S-H gel deterioration and enlarged porosity from PP fiber vaporization. A robust linear correlation with an R^2 value of 0.96 effectively illustrated the temperature-dependent compressive strength decline.
2. The bending strength of Engineered Cementitious Composite (ECC) consistently decreased with rising temperatures, unlike the less pronounced declines in compressive strength. A more significant percentage reduction was notably observed at 400 °C and 600 °C. Among the tests, a linear relationship with temperature exhibited the highest accuracy, with an R^2 value of 0.99. Following exposure to 400 °C and 600 °C, the remaining flexural strengths experienced significant decreases, falling to approximately 62% and 41%, respectively.
3. After exposure to 200 °C, ECC samples exhibited slight declines in the cracking number (N_{cr}), retaining approximately 98% of the original value, with more substantial decreases at higher temperatures. In contrast, Normal Concrete (NC) deteriorated more rapidly. ECCs maintained residual N_{cr} percentages of about 48% and 21% after exposure to 400 °C and 600 °C, while NC showed percentages of around 7% and 4% for the same temperatures. The heated ECC specimens, with finer matrix, increased binder content, and no aggregate, demonstrated superior impact endurance until cracking as related to NC.
4. The unheated ECC samples showed several impacts leading to failure significantly surpassing the corresponding N_{cr}, confirming the efficiency of ECCs with a dense and fine

microstructure, coupled with PP-fiber crack bridging elements, in enhancing impact energy absorption at the failure point. The retained Nf reached 260, approximately 4.33 times greater than that of NC, despite NC having a higher Ncr. Following exposure to 200 °C, ECC maintained nearly the same unheated Nf (99%), while NC retained only 23% of its original failure number when unheated. However, both NC and ECC experienced a substantial decrease in impact resistance following exposure to temperatures of 400 °C and 600 °C, resulting in the remaining Nf values dropping to levels below 4% and 10%, respectively for ECC Specimens indicating a significant reduction in impact resistance due to the high temperature exposure.

5. The linear relationship effectively depicted the decline in N_{cr} with temperature, showing a strong R^2 of 0.92. However, it inaccurately predicted N_f at 200 °C, underestimating it, and at 400 °C, overestimating it, resulting in a lower R^2 of 0.83. In contrast, the exponential relationship proved more suitable for describing the decrease in N_f with increased temperatures, achieving an R^2 of 0.83.
6. ECC outperforms normal concrete in all durability tests. After 90 days of sulphate curing, ECC specimens had a compressive strength loss of 24.6%, compared to 31.5% for normal concrete. For specimens exposed to 1% sulfuric acid, ECC showed a 26% strength loss versus 36% for normal concrete. ECC absorbed less water and had fewer pores, as indicated by sorptivity tests. Additionally, ECC demonstrated the highest resistance to chloride permeability compared to normal concrete.

9. Environmental Impact Assessment of ECCs in Solid Waste Management:

1. **Resource Depletion and Carbon Emissions Reduction:** ECCs often integrate recycled materials and SCMs like fly ash or slag, decreasing the need for new aggregates and cement. This minimizes resource depletion and reduces carbon emissions during ECC production compared to regular concrete. Life cycle assessments (LCAs) can assess ECCs' environmental benefits across their entire lifecycle, from raw material extraction to disposal.

2. **Reduction in Maintenance Needs and Resource Consumption:** ECCs' improved durability and crack resistance reduce maintenance needs and prolong service life in waste management facilities, cutting resource use over their lifecycle due to fewer repairs. Comparative assessments of ECC and traditional concrete structures can quantify environmental gains, including lower material extraction, transportation, and energy usage.
3. **Minimized Environmental Degradation:** ECCs' exceptional durability and chemical resistance render them ideal for challenging waste management settings. They endure exposure to acidic leachate, abrasive waste, and high temperatures in landfills, transfer stations, and recycling facilities without notable deterioration. Environmental evaluations gauge ECCs' performance over time, considering structural integrity, environmental harmony, and potential leaching into soil and groundwater.
4. **Case Studies and Real-World Examples:** Analyzing case studies and field data offers valuable insights into ECCs' environmental impact on waste management. Researchers can evaluate ECC installations alongside conventional concrete structures, assessing environmental pros and cons. Field studies involve long-term monitoring to gauge ECCs' resilience to environmental factors and measure indicators like carbon footprint, energy use, and waste generation.

Assessing ECCs' environmental impact in waste management is crucial for gauging sustainability and pinpointing areas for enhancement. By measuring ECCs' environmental advantages and mitigating potential drawbacks, stakeholders can decide wisely on ECC adoption, fostering sustainable and robust waste management approaches.

10. Potential Limitations and Challenges:

1. **Cost Considerations:** Due to specialized materials and production, ECCs have higher initial costs than conventional concrete. Cost-effectiveness studies are needed to assess the long-term benefits of waste management projects and justify the investment.

2. **Material Compatibility:** ECCs may not be suitable for all waste management applications due to specific material compatibility requirements. For instance, ECCs in facilities dealing with hazardous or corrosive waste must undergo thorough selection and testing to prevent material degradation and structural failure over time.
3. **Long-Term Performance:** While ECCs offer superior durability, their long-term performance in harsh waste management environments needs further investigation. Factors such as prolonged exposure to acidic or alkaline waste, abrasive materials, and high-temperature conditions can potentially degrade ECCs over time, impacting their structural integrity and effectiveness.
4. **Construction Practices:** Proper construction practices are essential for realizing the full potential of ECCs in waste management infrastructure. Challenges may arise in ensuring uniform mixing and placement of ECC materials, as well as achieving adequate curing and consolidation to optimize material properties and performance.

11. Future Research Directions:

1. **Cost-Effectiveness Studies:** Future research should prioritize conducting thorough cost-benefit analyses to evaluate ECCs' long-term economic viability in waste management. This involves assessing lifecycle expenses, maintenance savings, and environmental advantages to offer stakeholders a clearer view of ECC implementation's economic feasibility.
2. **Material Development:** Ongoing research is critical for enhancing ECC materials' chemical resistance and durability. Exploring various fiber types, binder compositions, and reinforcement methods can create ECC formulations optimized for waste management, addressing compatibility and long-term performance issues.
3. **Performance Monitoring and Evaluation:** Extended field studies and performance monitoring are necessary to evaluate ECCs' behavior in waste management facilities, including structural integrity, durability, and environmental compatibility, informing maintenance strategies, and identifying degradation mechanisms.

4. **Construction Best Practices:** Research efforts should concentrate on establishing standardized construction guidelines for ECC in waste management, covering material selection, mixing, placement, curing, and quality control to maximize ECC structure performance and lifespan.

By addressing these challenges and pursuing future research directions, the use of ECCs in waste management can be optimized, leading to more sustainable and resilient waste management practices.

References

Abid, S. R., Abdul-Hussein, M. L., Ayoob, N. S., Ali, S. H., and Kadhum, A. L. (2020a), Repeated drop-weight impact tests on self-compacting concrete reinforced with micro-steel fiber, *Heliyon*, **6**(1), e03198.

Abid, S. R., Hussein, M. L. A., Ali, S. H., and Ala'a, F. K. (2020b), Suggested modified testing techniques to the ACI 544-R repeated drop-weight impact test, *Construction and Building Materials*, **244**, 118321.

Abid, S. R., Ali, S. H., Goaiz, H. A., Al-Gasham, T. S., and Kadhim, A. L. (2021a), Impact resistance of steel fiber-reinforced self-compacting concrete, *Magazine of Civil Engineering (2712-8172)*, **105**(5).

Abid, S. R., Gunasekaran, M., Ali, S. H., Kadhum, A. L., Al-Gasham, T. S., Fediuk, R., Vatin, N., and Karelina, M. (2021b), Impact performance of steel fiber-reinforced self-compacting concrete against repeated drop weight impact, *Crystals*, **11**(2), 91.

Abrams, M. S. (1971), Compressive strength of concrete at temperatures to 1600F, *Special Publication*, **25**, 33-58.

ACI 544-2R, Measurement of Properties of Fiber Reinforced Concrete, American Concrete Institute: Detroit, MI, USA, 1999.

Albrektsson, J., Flansbjer, M., Lindqvist, J. E., and Jansson, R. (2011), Assessment of concrete structures after fire, *SP Technical Research Institute of Sweden,* Fire Technology SP Report No. 2011:19.

Alimrani, N. S., and Balazs, G. L. (2020), Investigations of direct shear of one-year old SFRC after exposed to elevated temperatures, *Construction and Building Materials*, **254**, 119308.

Al-Owaisy, S. R. (2007), Effect of high temperatures on shear transfer strength of concrete, *Journal of Engineering and Sustainable Development*, **11**(1), 92-103.

Arna'ot, F. H., Abbass, A. A., Abualtemen, A. A., Abid, S. R., and Özakça, M. (2017a), Residual strength of high strength concentric column-SFRC flat plate exposed to high temperatures, *Construction and Building Materials*, **154**, 204-218.

Arna'ot, F. H., Abid, S. R., Özakça, M., and Tayşi, N. (2017b), Review of concrete flat plate-column assemblies under fire conditions, *Fire Safety Journal*, **93**, 39-52.

Aslani, F., and Wang, L. (2019), Fabrication and characterization of an engineered cementitious composite with enhanced fire resistance performance, *Journal of Cleaner Production*, **221**, 202-214.

ASTM C1202-2017. Standard test method for electrical indication of concrete's ability to resist cementitious composites (ECC) under sulphate and chloride environment, Construction and Building Materials, Vol.133, pp.171-181.

ASTM C1585-2004. Standard test method for measurement of rate of absorption of water by hydraulic-cement concretes, American Society for Testing and Materials, USA.

ASTM C642-1997. Standard test Method for density, absorption, and voids in hardened concrete, American Society for Testing and Materials, USA.

Babalola, O. E., Awoyera, P. O., Le, D. H., and Romero, L. B. (2021), A review of residual strength properties of normal and high strength concrete exposed to elevated temperatures: Impact of materials modification on behaviour of concrete composite, *Construction and Building Materials*, **296**, 123448.

Çavdar, A. (2012), A study on the effects of high temperature on mechanical properties of fiber reinforced cementitious composites, *Composites Part B: Engineering*, **43**(5), 2452-2463.

Cheng, F. P., Kodur, V. K. R., and Wang, T. C. (2004), Stress-strain curves for high strength concrete at elevated temperatures, *Journal of Materials in Civil Engineering*, **16**(1), 84-90.

Chu, H. Y., Jiang, J. Y., Sun, W., and Zhang, M. (2016), Mechanical and physicochemical properties of ferro-siliceous concrete subjected to elevated temperatures, *Construction and Building Materials*, **122**, 743-752.

Deng, Z. H., Huang, H. Q., Ye, B., Wang, H., and Xiang, P. (2020), Investigation on recycled aggregate concretes exposed to high temperature by biaxial compressive tests, *Construction and Building Materials*, **244**, 118048.

Drzymala, T., Jackiewicz-Rek, W., Tomaszewski, M., Kuś, A., Gałaj, J., and Šukys, R. (2017), Effects of high temperature on the properties of High-Performance Concrete (HPC), *Procedia Engineering*, **172**, 256-263.

Düğenci, O., Haktanir, T., and Altun, F. (2015), Experimental research for the effect of high temperature on the mechanical properties of steel fiber-reinforced concrete, *Construction and Building Materials*, **75**, 82-88.

Guo, Y. C., Zhang, J. H., Chen, G. M., and Xie, Z. H. (2014), Compressive behaviour of concrete structures incorporating recycled concrete aggregates, rubber crumb and reinforced with steel fibre, subjected to elevated temperatures, *Journal of cleaner production*, **72**, 193-203.

Husem, M. (2006), The effects of high temperature on compressive and flexural strengths of ordinary and high-performance concrete, *Fire Safety Journal*, **41**(2), 155-163.

Ismail, M. K., and Hassan, A. A. (2017), Impact resistance and mechanical properties of self-consolidating rubberized concrete reinforced with steel fibers, *Journal of Materials in Civil Engineering*, **29**(1), 04016193.

Ismail, M. K., Hassan, A. A., and Lachemi, M. (2019), Performance of self-consolidating engineered cementitious composite under drop-weight impact loading, *Journal of materials in civil Engineering*, **31**(3), 04018400.

IS: 516–1959. (1979). Indian Standard Code of Practice-Methods of Test for Strength of Concrete, Bureau of Indian Standards, New Delhi.

IS: 9103–1999. Indian Standard Code of Practice- Concrete Admixtures: Specification, Bureau of Indian Standards, New Delhi.

Jabir, H. A., Abid, S. R., Murali, G., Ali, S. H., Klyuev, S., Fediuk, R., Vatin, N., Promakhov, V. and Vasilev, Y. (2020), Experimental tests and reliability analysis of the cracking impact resistance of UHPFRC, *Fibers*, **8**(12), 74.

Li, V.C. (1993), From micromechanics to structural engineering- The design of cementitious composites for civil engineering applications, *Journal of Structural Mechanics and Earthquake Engineering*, **10**(2), 37–48.

Li, V.C. Engineering Cementitious Composites (ECC)-Materials, Structural, and Durability Performance; University of Michigan: Ann Arbor, MI, USA, 2007.

Li, Q., Gao, X., Xu, S., Peng, Y., and Fu, Y. (2016), Microstructure and mechanical properties of high-toughness fiber-reinforced cementitious composites after exposure to elevated temperatures, *Journal of materials in civil engineering*, **28**(11), 04016132.

Li, Q. H., Sun, C. J., and Xu, S. L. (2019), Thermal and mechanical properties of ultrahigh toughness cementitious composite with hybrid PVA and steel fibers at elevated temperatures, *Composites Part B: Engineering*, **176**, 107201.

Liu, J. C., Tan, K. H., and Fan, S. (2018), Residual mechanical properties and spalling resistance of strain-hardening cementitious composite with Class C fly ash, *Construction and Building Materials*, **181**, 253-265.

Mahakavi, P., and Chithra, R. (2019), Impact resistance, microstructures and digital image processing on self-compacting concrete with hooked end and crimped steel fiber, *Construction and Building Materials*, **220**, 651-666.

Mastali, M., and Dalvand, A. (2016), The impact resistance and mechanical properties of self-compacting concrete reinforced with recycled CFRP pieces. *Composites Part B: Engineering*, **92**, 360-376.

Murali, G., Asrani, N.P., Ramkumar, V.R., Siva, A., and Haridharan, M.K. (2019), Impact Resistance and Strength Reliability of Novel Two-Stage Fibre-Reinforced Concrete, *Arabian Journal for Science and Engineering*, **44**, 4477–4490.

Murali, G., Abid, S.R., Mugahed Amran, Y.H., Abdelgader, H.S., Fediuk, R., Susrutha, A., and Poonguzhali, K. (2020), Impact performance of novel multi-layered prepacked aggregate fibrous composites under compression and bending, *Structures*, **28**, 1502–1515.

Murali, G., Abid, S.R., Abdelgader, H.S., Amran, M.Y.H., Shekarchi, M., and Wilde, K. (2021a), Repeated projectile impact tests on multi-layered fibrous cementitious composites, *International Journal of Civil Engineering*, **19**, 635–651.

Murali, G., Abid, S. R., Amran, M., Fediuk, R., Vatin, N., and Karelina, M. (2021b), Combined effect of multi-walled carbon nanotubes, steel fibre and glass fibre mesh on novel two-stage expanded clay aggregate concrete against impact loading, *Crystals*, **11**(7), 720.

Murali, G., Abid, S.R., Karthikeyan, K., Haridharan, M.K., Amran, M., and Siva, A. (2021c), Low-velocity impact response of novel prepacked expanded clay aggregate fibrous concrete produced with carbon nano tube, glass fiber mesh and steel fiber, *Construction and Building Materials*, **284**, 122749.

Netinger, I., Kesegic, I., and Guljas, I. (2011), The effect of high temperatures on the mechanical properties of concrete made with different types of aggregates, *Fire safety journal*, **46**(7), 425-430.

Nili, M., and Afroughsabet, V. (2010), Combined effect of silica fume and steel fibers on the impact resistance and mechanical properties of concrete, *International journal of impact engineering*, **37**(8), 879-886.

Phan, L. T., and Carino, N. J. (1998), Review of mechanical properties of HSC at elevated temperature, *Journal of Materials in Civil Engineering*, **10**(1), 58-65.

Phan, L. T., and Carino, N. J. (2003), Code provisions for high strength concrete strength-temperature relationship at elevated temperatures, *Materials and Structures*, **36**, 91-98.

Poon, C. S., Shui, Z. H., and Lam, L. (2004), Compressive behavior of fiber reinforced high-performance concrete subjected to elevated temperatures, *Cement and concrete Research*, **34**(12), 2215-2222.

Prasad, N. and Murali, G. (2021), Exploring the impact performance of functionally-graded preplaced aggregate concrete incorporating steel and polypropylene fibres, *Journal of Building Engineering*, **35**, 102077.

Rafiei, P., Shokravi, H., Mohammadyan-Yasouj, S. E., Koloor, S. S. R., and Petrů, M. (2021), Temperature impact on engineered cementitious composite containing basalt fibers, *Applied Sciences*, **11**(15), 6848.

Ramakrishnan, K., Depak, S., Hariharan, K., Abid, S.R., Murali, G., Cecchin, D., Fediuk, R., Amran, Y.M., Abdelgader, H.S., and Khatib, J.M. (2021), Standard and modified falling mass impact tests on preplaced aggregate fibrous concrete and slurry infiltrated fibrous concrete, *Construction and Building Materials*, **298**, 123857.

Ramkumar, V. R., Murali, G., Asrani, N. P., and Karthikeyan, K. (2019), Development of a novel low carbon cementitious two stage layered fibrous concrete with superior impact strength, *Journal of Building Engineering*, **25**, 100841.

Roufael, G., Beaucour, A. L., Eslami, J., Hoxha, D., and Noumowé, A. (2021), Influence of lightweight aggregates on the physical and mechanical residual properties of concrete subjected to high temperatures, *Construction and Building Materials*, **268**, 121221.

Sahmaran, M., Lachemi, M., and Li, V. (2010), Assessing mechanical properties and microstructure of fire-damaged engineered cementitious composites, *ACI Materials Journal*, **107**, 297–304.

Şahmaran, M., Özbay, E., Yücel, H. E., Lachemi, M., and Li, V. C. (2011), Effect of fly ash and PVA fiber on microstructural damage and residual properties of engineered cementitious composites exposed to high temperatures, *Journal of materials in civil engineering*, **23**(12), 1735-1745.

Salaimanimagudam, M. P., Suribabu, C. R., Murali, G., and Abid, S. R. (2020), Impact response of hammerhead pier fibrous concrete beams designed with topology optimization, *Periodica Polytechnica Civil Engineering*, **64**(4), 1244-1258.

Shallal, M. A., and Al-Owaisy, S. R. (2007), Strength and elasticity of steel fiber reinforced concrete at high temperatures, *Journal of Engineering and Sustainable Development*, **11**(2), 125-133.

Shang, X., and Lu, Z. (2014), Impact of high temperature on the compressive strength of ECC, *Advances in Materials Science and Engineering*, **2014**, 919078.

Sultan, H. K., and Alyaseri, I. (2020), Effects of elevated temperatures on mechanical properties of reactive powder concrete elements, *Construction and Building Materials*, **261**, 120555.

Torić, N., Boko, I., and Peroš, B. (2013), Reduction of postfire properties of high-strength concrete, *Advances in Materials Science and Engineering*, **2013**, 712953.

Tufail, M., Shahzada, K., Gencturk, B., and Wei, J. (2017), Effect of elevated temperature on mechanical properties of limestone, quartzite and granite concrete, *International Journal of Concrete Structures and Materials*, **11**(1), 17-28.

Wang, W., and Chouw, N. (2017), The behaviour of coconut fibre reinforced concrete (CFRC) under impact loading, *Construction and Building Materials*, **134**, 452-461.

Wang, Z. B., Han, S., Sun, P., Liu, W. K., and Wang, Q. (2021), Mechanical properties of polyvinyl alcohol-basalt hybrid fiber engineered cementitious composites with impact of elevated temperatures, *Journal of Central South University*, **28**(5), 1459-1475.

Zhihui, Y. U., Zhen, Y. U. A. N., Chaofan, X. I. A., and Zhang, C. (2020), High temperature flexural deformation properties of engineered cementitious composites (ECC) with hybrid fiber reinforcement, *Research and Application of Materials Science*, **2**(2), 17-26.